



RESEARCH

Open Access

Finding of widespread viral and bacterial revolution dsDNA translocation motors distinct from rotation motors by channel chirality and size

Gian Marco De-Donatis^{1,2,3†}, Zhengyi Zhao^{1,2,3†}, Shaoying Wang^{1,2,3}, Lisa P Huang⁴, Chad Schwartz^{1,2,3}, Oleg V Tsodikov², Hui Zhang^{1,2,3}, Farzin Haque^{1,2,3} and Peixuan Guo^{1,2,3,5*}

Abstract

Background: Double-stranded DNA translocation is ubiquitous in living systems. Cell mitosis, bacterial binary fission, DNA replication or repair, homologous recombination, Holliday junction resolution, viral genome packaging and cell entry all involve biomotor-driven dsDNA translocation. Previously, biomotors have been primarily classified into linear and rotational motors. We recently discovered a third class of dsDNA translocation motors in Phi29 utilizing revolution mechanism without rotation. Analogically, the Earth rotates around its own axis every 24 hours, but revolves around the Sun every 365 days.

Results: Single-channel DNA translocation conductance assay combined with structure inspections of motor channels on bacteriophages P22, SPP1, HK97, T7, T4, Phi29, and other dsDNA translocation motors such as bacterial FtsK and eukaryotic mimiviruses or vaccinia viruses showed that revolution motor is widespread. The force generation mechanism for revolution motors is elucidated. Revolution motors can be differentiated from rotation motors by their channel size and chirality. Crystal structure inspection revealed that revolution motors commonly exhibit channel diameters larger than 3 nm, while rotation motors that rotate around one of the two separated DNA strands feature a diameter smaller than 2 nm. Phi29 revolution motor translocated double- and tetra-stranded DNA that occupied 32% and 64% of the narrowest channel cross-section, respectively, evidencing that revolution motors exhibit channel diameters significantly wider than the dsDNA. Left-handed oriented channels found in revolution motors drive the right-handed dsDNA via anti-chiral interaction, while right-handed channels observed in rotation motors drive the right-handed dsDNA via parallel threads. Tethering both the motor and the dsDNA distal-end of the revolution motor does not block DNA packaging, indicating that no rotation is required for motors of dsDNA phages, while a small-angle left-handed twist of dsDNA that is aligned with the channel could occur due to the conformational change of the phage motor channels from a left-handed configuration for DNA entry to a right-handed configuration for DNA ejection for host cell infection.

Conclusions: The revolution motor is widespread among biological systems, and can be distinguished from rotation motors by channel size and chirality. The revolution mechanism renders dsDNA void of coiling and torque during translocation of the lengthy helical chromosome, thus resulting in more efficient motor energy conversion.

Keywords: DNA translocase, DsDNA viruses, Viral DNA packaging motor, Viral assembly, Bacteriophage, DNA helicase, Revolution force, Phi29, FtsK, RecA, Nanomotor

* Correspondence: peixuan.guo@uky.edu

†Equal contributors

¹Nanobiotechnology Center, University of Kentucky, Lexington, KY, USA

²Department of Pharmaceutical Sciences, College of Pharmacy, University of Kentucky, Lexington, KY, USA

Full list of author information is available at the end of the article

Background

Transportation of dsDNA from one cellular compartment to another is a prevalent process in all living systems. Many members of the ASCE (Additional Strand Catalytic E) superfamily are nanomotors with a hexameric arrangement of subunits that facilitate a wide range of functions, including dsDNA riding, tracking, packaging, and translocation, which are critical to many processes such as DNA repair, replication, recombination, chromosome segregation, transcription, and cellular reorganization [1,2]. Despite their functional diversity, a common feature of the motors of this family is their ability to convert energy obtained from the binding or hydrolysis of ATP into mechanical energy which results in local/global protein unfolding, complex assembly/disassembly, or grabbing/pushing dsDNA for translocation [1-11]. The hexagonal shape of the motor facilitates bottom-up assembly in nanomachine manufacturing [12-20].

Nanobiomotors have previously been classified into two main categories: linear and rotational motors, which have been clearly documented using single-molecule imaging and X-ray crystallography [21-26]. During replication, dsDNA viruses translocate their genomic DNA into preformed protein shells (procapsids) [27-33]. This entropically

unfavorable process is accomplished by a nanomotor that uses ATP as an energy source [34-42]. This dsDNA packaging motor consists of a connector channel and packaging molecules to carry out its activities. For 35 years, it has been popularly believed that DNA packaging in dsDNA viruses involves rotation motors [43], which is seemingly supported by the swivel structure in the crystal structures of all connector channels of bacteriophages [44-46]. However, extensive investigations revealed that the dsDNA packaging motor channels do not rotate during motor actions [47-51]. For example, the T4 DNA-packaging motor remains active when the motor channel protein is crosslinked to the protein shell [47]. Single-molecule imaging further verified that there is no rotation of the channel during packaging [48]. These evidences have brought up a puzzle concerning how packaging can involve a rotation motor without any rotating components. In 2010, another question was raised regarding the inverse orientations of the Phi29 motor channel and dsDNA helices [52], which further questioned the involvement of rotational motion, since the rotation mechanism of dsDNA as a bolt threading onto a motor channel as a nut requires that the threads of the bolt and the nut have the same directionality. Recently, we have discovered that

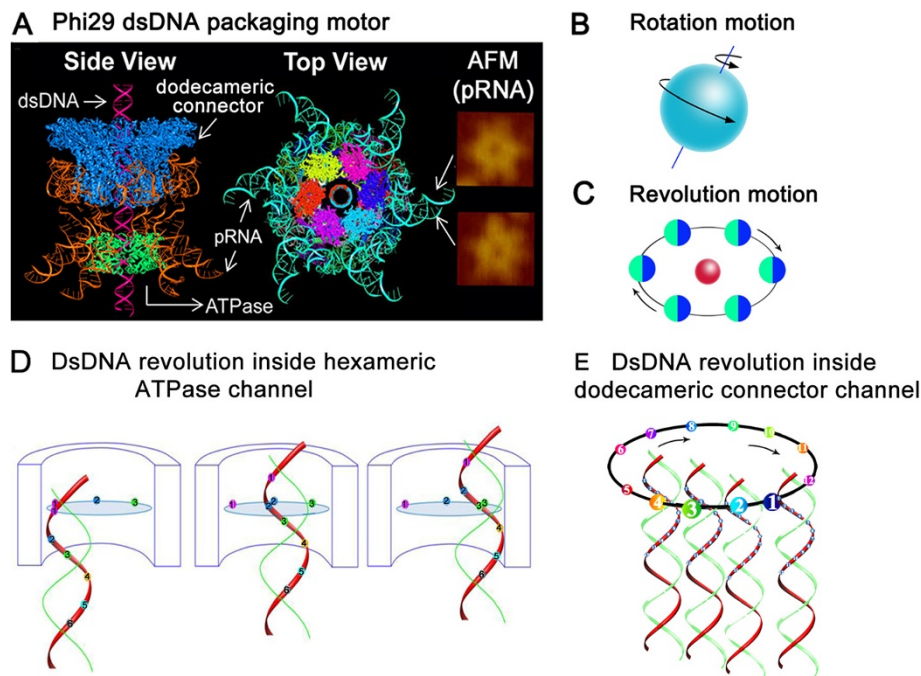


Figure 1 Illustration of rotation motions and revolution motions using Phi29 revolution motor as an example. (A) 3D structure of Phi29 dsDNA packaging motor in a side view and top view with a pRNA hexamer derived from the crystal structure [16], and the AFM images of the pRNA hexamer with extended loops. (B) Illustration of rotation motions like the Earth *rotates* around its own axis. (C) Illustration of revolution motions like the Earth *revolves* around the Sun without rotation. (D) Illustration of the dsDNA revolution inside the hexameric ATPase channel. Only three of the six steps are shown. (E) Illustration of the dsDNA revolution inside the dodecameric connector channel, only four of the twelve steps are shown. Neither the channel nor the dsDNA needs to rotate during the revolution through channels (for animation, see http://nanobio.uky.edu/Connector-DNA_revolution.wmv).

bacteriophage Phi29 dsDNA packaging motor uses a revolution mechanism without rotation, coiling, or torque forces (Figure 1) [9,50,53,54]. The hexameric ATPase ring exercises a force to push the dsDNA through the dodecamer channel acting as a one-way valve [9,10,52]. Observation of this revolution mechanism establishes a third class of biomotors. This finding resolves many puzzles throughout the history of long-lasting studies on the motor [9,10,55].

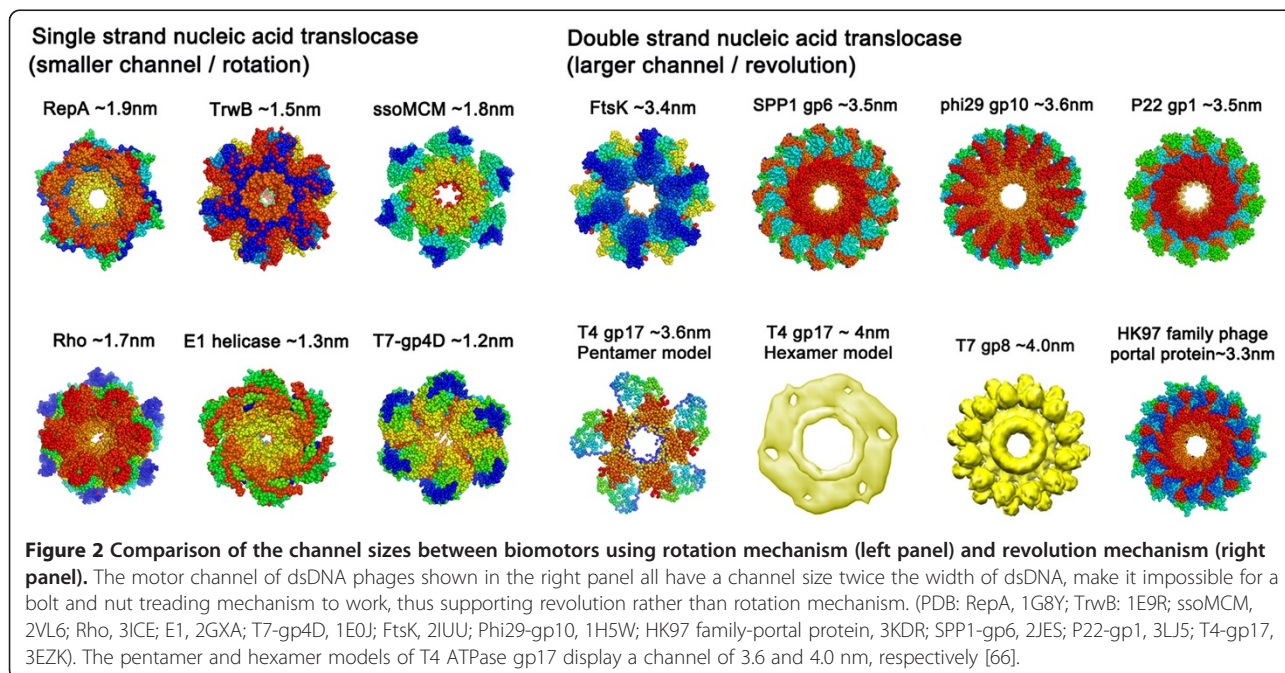
As the translocation of dsDNA is a ubiquitous process in living systems, and motors of all dsDNA bacteriophages share some common structural and functional features, we aimed at determining whether the revolution model discovered in Phi29 can generally be applied to other DNA packaging motors. Cellular counterparts that show a strong similarity to the Phi29 viral DNA packaging motor are the FtsK and SpoIIIE family motors, featuring a hexameric motor that transports DNA and separates the intertwined lengthy genomic dsDNA during cell division or binary fission [56-63]. Unwinding of the supercoiled dsDNA resulting from rotation would lead to expensive energy consumption [64]. The revolution mechanism adopted by biological systems during evolution, resembles an optimized mechanism for translocation of lengthy dsDNA genome without coiling. In this report, we analyze the motor mechanism regarding force generation of Phi29 and compare its structure and mechanism to that of DNA packaging motors of SPP1, P22, T7, HK97, mimivirus, and vaccinia virus, as well as some cellular proteins such as FtsK and SpoIIIE. We also provide a simple way to distinguish between revolution and rotation motors by channel size and chirality.

Results and discussion

Revolution and rotation motors can be distinguished by motor channel size

Previous observations that only one subunit of the hexamer binds to dsDNA at a time [8,50], as well as the cooperativity and sequential action among hexameric ATPase subunits [8], confirmed the revolution of dsDNA along the channel [50]. In this revolution process, dsDNA advances by sliding along the channel wall instead of proceeding through the center of the channel. Thus, the channel would be expected to be wider than the diameter of the dsDNA to ensure sufficient space for revolution. Inspection of the motor channel size in available crystal structures and cryo-EM data confirmed this expectation; while the width of dsDNA is 2 nm, the diameters of the narrowest region of the connector channels of Phi29 [46], SPP1 [65], HK97, the ATPase ring of T4 [66], as well as the dsDNA translocase FtsK [60] of bacteria, are all larger than 3 nm (Figure 2).

On the other hand, the channels of rotation motors, such as replicative DNA helicases TrwB, E1, and DnaB [67-69], are smaller than 2 nm in diameter (Figure 2). For rotation motors, the channel would thus be expected to have a similar width as the ssDNA to allow for the bolt and nut threading mechanism. Nonetheless, during some processes for certain rotation motors, only one strand enters the channel while the other remains outside [5,64,67-71]. In these situations, local unwinding fluctuations of the dsDNA might cause separation of the two strands and facilitate the threading of the ssDNA strand into the center of the hexameric ring, as suggested by smFRET experiments [72-74]. It has been reported that the ssDNA



within the channel displays an A form helical structure [69], thus the channel diameter should be no larger than 2 nm to allow for contact between the DNA and the channel. The situation for branch migration is more complicated and beyond the scope of this manuscript. Overall, the above data indicates that the revolution motor can be distinguished from the rotation motor by the size of the motor channel.

Conductance assay of single connector channels for translocation of tetra-stranded DNA reveals a three-fold width of Phi29 channels compared to dsDNA

The channel size was further assessed by single-channel conductance assays using Phi29 connector channels as a model system. A current blockage of 32% was observed for translocation of dsDNA through the connector channel (Figure 3A), consistent with the ratio of the cross-sectional areas of dsDNA ($(2/2)^2 \times 3.14 = 3.14 \text{ nm}^2$) and channel ($((3.6/2)^2 \times 3.14 = 10.2 \text{ nm}^2$, $10.2 \text{ nm}^2 \div 3.14 \text{ nm}^2 = 32\%$). For tetra-stranded DNA, which was constructed by DNA nanotechnology (Materials and methods) (Haque F, Wang S, Stites C, Chen L, Wang C, Guo P: Single pore translocation of folded, double-stranded, and tetra-stranded DNA through channel of bacteriophage Phi29 DNA packaging motor, submitted), when passing through the connector channel, a blockage of ~64% was observed (Figure 3B). Thus, the cross-sectional area at the narrowest region of the Phi29 connector funnel is three-fold the area of the dsDNA. Such a big channel size makes it impossible for a bolt and nut tracing mechanism, and makes it likely that only one ATPase subunit at a time can bind to dsDNA [8,50].

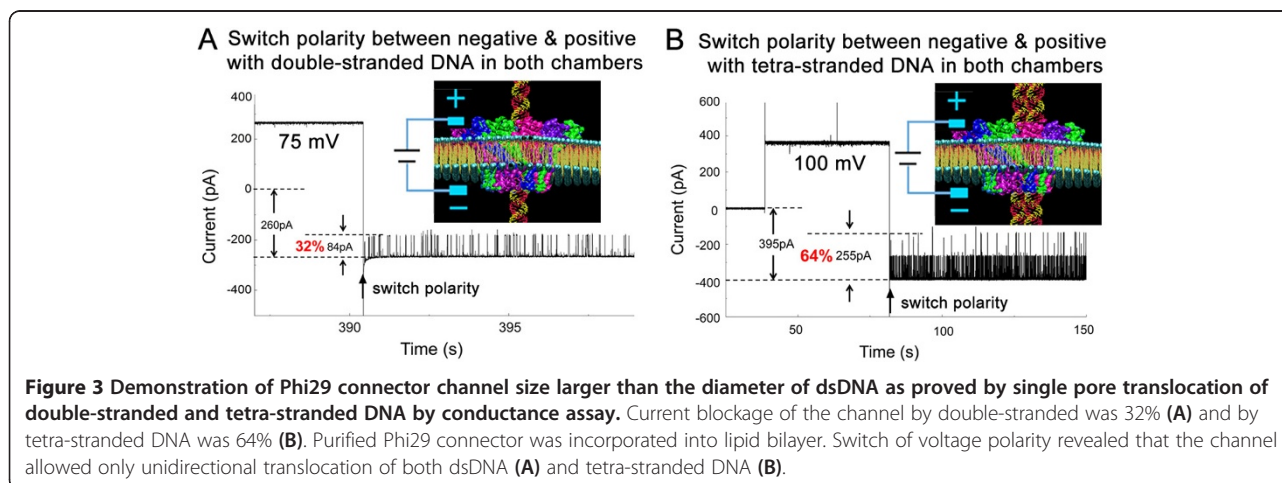
Both dsDNA and tetra-stranded DNA show one-way translocation through the Phi29 motor channel, since the switch of the electrical polarity changed the dsDNA from passable to impassable or vice versa through the channel (Figure 3). One-way traffic of tetra-stranded DNA reveals that the channel does not merely serve as a

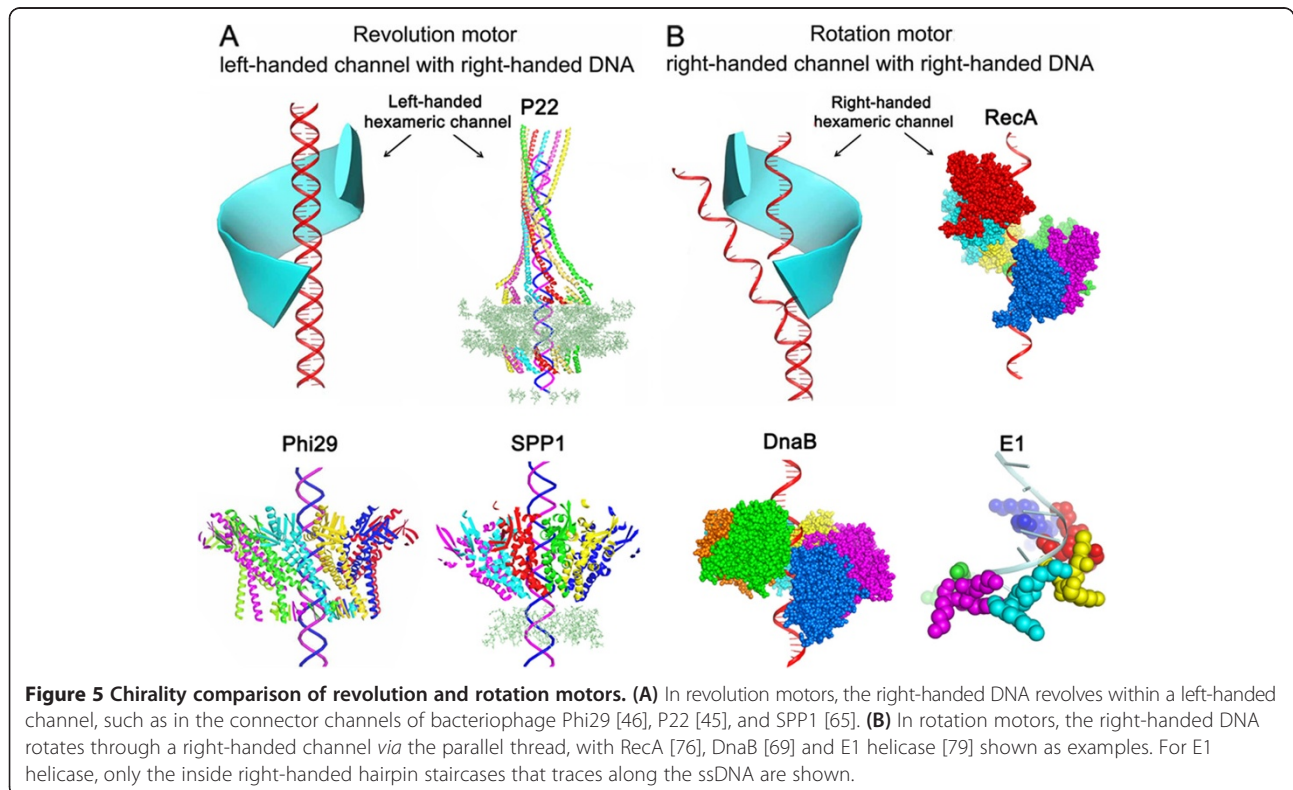
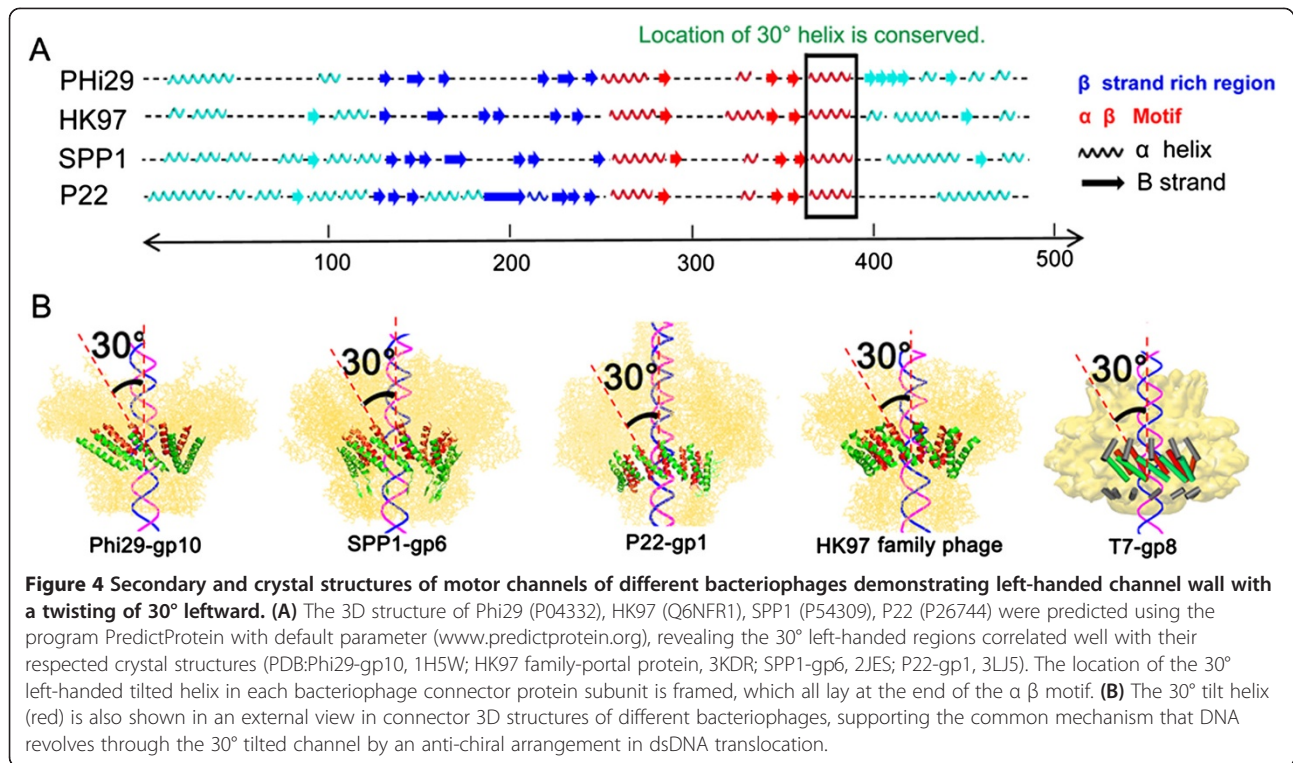
pathway, it plays an active role by forming contacts with translocating double- and tetra-stranded DNA.

The left-handed chirality of revolution motors is distinct from the right-handed chirality of rotation motors

From mechanistic and physical standpoints, revolution motors depend upon a left-handed channel while rotation motors require a right-handed channel, to match the right-handed orientation seen in both B-type DNA and A-type DNA helices. Recently, it has been reported that the anti-chiral arrangement between the Phi29 channel and the dsDNA helices facilitates the revolution of the dsDNA for uni-directional translocation during packaging [50,54]. Analysis of the crystal structures of the motor channel of SPP1 [65], T7 [75], HK97, P22 [45], and Phi29 [46] revealed that all of these motor channels display the anti-chiral arrangement between the channel and the DNA helices. The helical domains of the 12 protein subunits aligned to form the connector channels in all of these phages are tilted at 30° left-handed relative to the vertical axis of the channel, resulting in a configuration that runs anti-chiral to the right-handed dsDNA helices during packaging (Figures 4 and 5A). This structural arrangement greatly facilitates the controlled motion, supporting the conclusion that dsDNA revolves, instead of rotating, through the connector channel without producing coiling or torsional forces while touching each of the 12 connector subunits in 12 discrete steps of 30° transitions for each contact [50].

Sequence alignments do not show apparent homology among the portal proteins of SPP1, T7, and HK97 family phages. Protein sizes also vary among different bacteriophages, ranging from 36 kDa (Phi29 gp10), 57 kDa (SPP1 gp6), 59 kDa (T7 gp8), to 94 kDa (P22 gp1) [44,75]. However, these portal proteins assemble into a propeller-like structure composed of 12 subunits with a central channel that acts as a valve for DNA translocation, and they all share very similar three-dimensional structures





with several conserved regions that serve a common function in DNA packaging. Secondary structure prediction was carried out in search of structural similarities. The predicted secondary structures matched almost perfectly with the known 3D arrangements, confirming the validity of the results. Among almost all of the portal proteins, a very similar pattern of strands and helices with comparable spacing and length (Figure 4A) was found, particularly a sequence of α - β - α - β - α stretch. Detailed analysis of quaternary structures has revealed that the 30° tilted helix exists in all portal proteins of P22, SPP1, Phi29, T7, and HK97 family phages (Figure 4B). Further mapping studies have revealed that the position of the 30° tilt in the quaternary structure is located at the same conserved sequence at the last alpha helix of the α - β - α - β - α stretch (Figure 4A), indicating that this 30° anti-chiral arrangement plays a critical role in dsDNA packaging as it has been conserved by evolution.

As aforementioned, the rotation motors should have a right-handed channel to ensure parallel threading to the right-handed DNA. Indeed, crystal structure studies of helicase-DNA complexes have verified the right-handed spiral configuration of the hexameric protein-DNA complex (Figure 5) [69,76,77]. In some cases, the motor channels adopt right-handed chirality only when the ring is distorted while in complex with DNA, such as RecA filament [76] and DnaB, which functions in a nonplanar hexameric conformation during their movement relative to DNA [69], otherwise, it remains as a closed symmetrical ring as observed in the absence of DNA [78]. E1 helicase also adopts a right handed staircase pattern in the conformation of side chains when bound with DNA [79]. All of these crystallographic studies suggest that these right-handed complexes use the rotation mechanism (or a mechanism similar to a rotation mechanism for RecA, where its monomers assemble on one end of the filament and disassemble on the other). It is also possible that the gp16 ATPase in the Phi29 dsDNA packaging motor also adopts a nonplanar filament assembled from continuously spiral hexamers (or assembled from dimers) rather than a planar closed ring during the DNA packaging, however, gp16 ring might display a left-handed configuration (Figure 5A).

Common force generation mechanism of dsDNA translocation motors in bacteria, eukaryotic and prokaryotic viruses

The recently discovered revolution motors use a hexameric ATPase to drive the advance of dsDNA in a sequential manner. Cellular dsDNA translocases also assemble into hexameric structures [4,5,80]. The cellular components that show the strongest similarity to phage revolution motors are found in the bacteria FtsK and SpoIIIE family of the ASCE DNA motor group [56-58,63]. Available

evidences [58,60] lead to our hypothesis that FtsK and SpoIIIE motors also use a revolution mechanism to translocate dsDNA without rotation. Indeed, translocation of dsDNA by FtsK at a rate of 1.6-1.75 base per ATP [58,60] quantitatively agrees with the Phi29 DNA packaging motor in which each ATPase subunit uses one ATP to package 1.75 nucleotide [9,34,50,53,54]. Sequence studies of motor components of large eukaryotic dsDNA viruses, such as *Acanthamoeba polyphaga mimivirus* (APMV), and vaccinia viruses contain a dsDNA translocation motor that is similar to that of the FtsK-HerA superfamily [63,81,82], suggesting that these viruses also use the revolution mechanism for dsDNA packaging. Computation studies provide strong evidence that Phi29 DNA packaging motor ATPase gp16, FtsK, and the mimivirus motor ATPase all fall into the FtsK-HerA superfamily with a configuration of a hexameric motor ring [63,81].

As shown in this report, quaternary structure analysis revealed that a left-handed, 30° tilted helix arrangement exists in the channel wall of dsDNA bacteriophages P22, SPP1, Phi29, T7, and HK97. During revolution of dsDNA through the channel, it advances by touching the side of the channel wall instead of proceeding through the center of the channel [50,83]. As a result, the 30° left-handed direction for each transition between two connector subunits and the 30° alteration for dsDNA to advance 1/12 of helical pitch neutrally, resulting in a zero gain, that is, no rotation occurs for the dsDNA during the translocation. The proposed model of 60° per step of the FtsK hexamer ($360^\circ \div 6 = 60^\circ$) [58] agrees with the finding of 30° per step within the dodecamer connector channel ($360^\circ \div 12 = 30^\circ$) of all dsDNA bacteriophages and 60° per steps within the Phi29 hexameric ATPase gp16 [9,50,53,54].

Channel size and chirality are key factors in the identification of translocation motor types which can reveal the motor mechanism. The channel size is a physical confinement that can be used to distinguish revolution motors from rotation motors. As shown in this report, examination of the motor structures from X-ray crystallography reveals that revolution motor channels are larger than rotation motor channels. The finding that heteroduplex loop structures up to 19 bases can translocate through the phage lambda portal with the same efficiency as genome packaging [84] is another indication that the channel of lambda is wider than the dsDNA as well.

Revolution motors make contact with only one strand of the dsDNA in the 5' to 3' direction in order to revolve along the connector channel, which has been evidenced in various motors such as Phi29 [85,86] and T4 [87]. The model that dsDNA interacts with the internal surface of the hexameric ring [50,54] is in agreement with the observation in FtsK that only one strand of the dsDNA touches the internal wall of the motor channel [57,58].

Besides, further analysis of the crystal structures of phage connectors among SPP1, P22, and Phi29 [46,54,88,89] revealed four potential-relaying electropositive lysine residues lying on the predominantly negatively charged connector channel surface. Although these four positively charged layers are nonessential for motor DNA packaging activity [89], they are reported to influence DNA translocation [89,90]. Investigations into the detailed interaction of lysine residues with the bacteriophage genome during translocation revealed that the force generation mechanism of the relaying layers inside the channel wall altered the speed of DNA translocation resulting in four pauses [9,54]. The interaction between these positively charge lysine rings and the negatively charged phosphate backbone of the DNA suggests that SPP1, P22 and Phi29 viral dsDNA packaging motors involve an electrostatic force in DNA translocation.

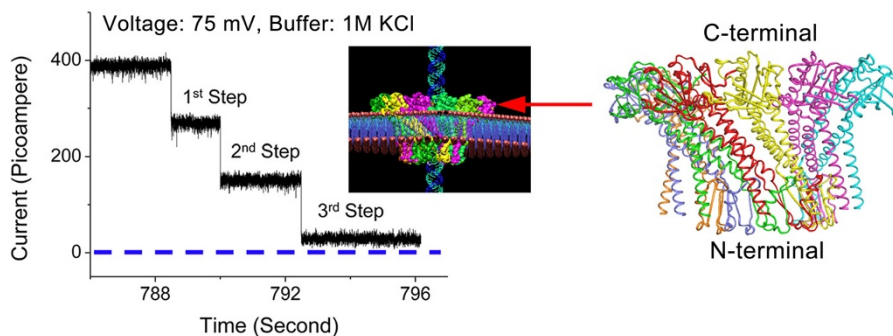
Furthermore, it has been reported that the dsDNA spooling in the filled capsid is a common phenomenon in all

the T7, Phi29, ϵ 15, P22, and λ phages [91-94]. The revolution mechanism explains this spooling phenomenon. During packaging of DNA [50,54], dsDNA will spool within the procapsid naturally as a result of the revolution process. Since rotation is not involved, no coiling is generated and no free DNA terminus is required during spooling. Initially, extra room results in a random arrangement of the entering DNA, however, towards completion of packaging it spools tighter and tighter due to revolution, which results in a more ordered orientation of the dsDNA [91-94]. In addition, the reported revolution mechanism of phage DNA packaging motors is also consistent with recent cryo-EM imaging studies showing that the T7 dsDNA core tilts from its central axis [83].

DNA twists rather than rotates due to motor channel conformational changes during DNA translocation

Many connector channels of dsDNA bacteriophages (Figure 4) adopt a left-handed channel wall to facilitate

A. Conformational changes of Phi29 connector channel detected by single channel conductance assay



B. Twist of DNA during Phi29 motor packaging resulting from the conformational changes of the connector channel

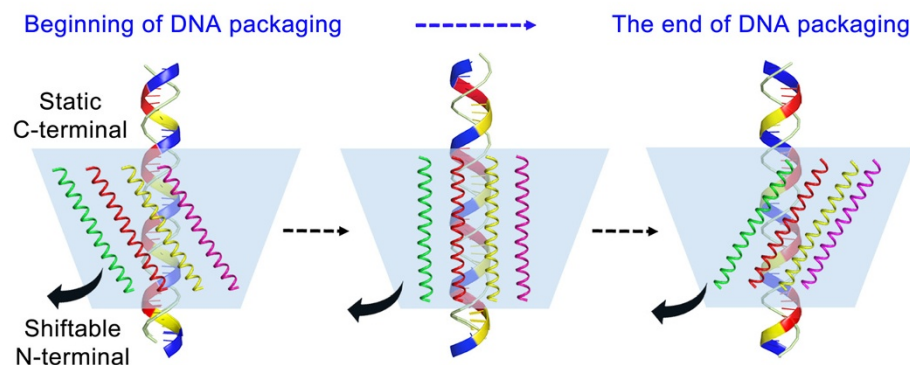


Figure 6 Illustration of the mechanism of dsDNA twisting during DNA packaging due to conformational changes of the Phi29 connector channel. (A) Discrete three step-wise conformational changes of Phi29 connector channel were detected by single channel conductance assay with the connector embedded in lipid bilayer. The external view of the crystal structure of the connector channel is shown on the right. **(B)** The C-terminal of the connector inside the procapsid is more static than the external N-terminal. As a result, the N-terminal of the connector may shift leftwards during the DNA packaging, leading to the clockwise twist of the DNA that aligns within the connector channel wall.

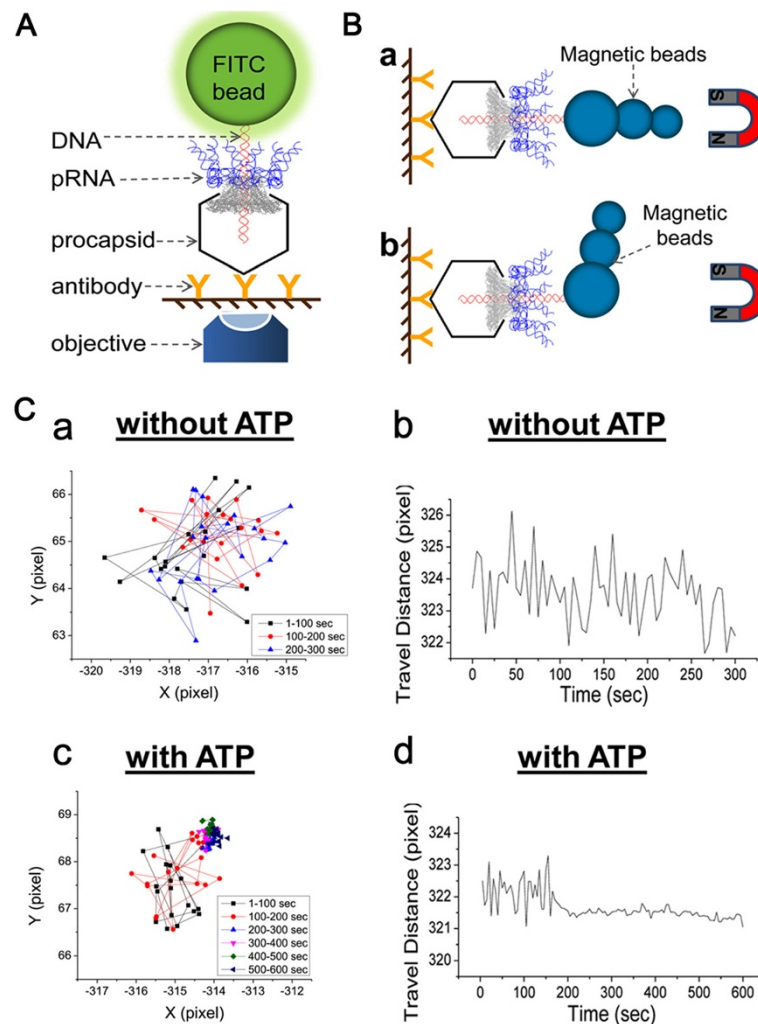


Figure 7 Demonstration of no DNA rotation by real-time direct observation of single motor DNA packaging. Procapsid was immobilized in glass and the distal end of dsDNA was tethered to a bead. DNA is packaged vertically (A) or horizontally (B) towards the slide surface (graphic is not drawn to scale). (C) The motion of the bead is tracked during DNA packaging without (a and b) and with (c and d) the addition of ATP to the sample. The motion of the bead ceased at later times only when ATP was added (c) and (d) due to the physical restriction of DNA being completely packaged. (a) and (c) show the trajectories of the bead. Different colors represent different time ranges during the translocation. (b) and (d) show the changes in beads travel distance versus time.

one-way traffic during dsDNA packaging into pre-assembled protein shells [52,54]. The conformational changes of the channel have been reported associated with this packaging process [95,96]. Such conformational changes allow conversion of the left-handed connector after completion of DNA packaging towards the opposite configuration, thus facilitating DNA one-way ejection into host cells for infection. Indeed, three steps of conformational changes of the Phi29 connector were detected (Figure 6A) [96], and discovered in the DNA packaging motor of SPP1 (Wang and Guo, unpublished data). Noticeable conformational differences between isolated Phi29 connectors and connectors in virions confirm such a structural

transition after DNA packaging [95]. In the Phi29 crystal structure, the connector subunit displays a left-handed 30° tilt (Figure 4). However, when treated as a rigid body, the crystal structure clearly does not fit into the cryo-EM density maps, indicated by a correlation coefficient as low as 0.55. After manual adjustments, the correlation coefficient was improved to 0.70, resulting in a 10° twist of the connector towards the connector axis [95]. On the other hand, the N-terminal external region is difficult to adjust to fit as a rigid body into other parts of the connector density. It was found that the N-terminal external region underwent significant conformational shift in the DNA-filled capsid [95]. It was concluded that angular twisting

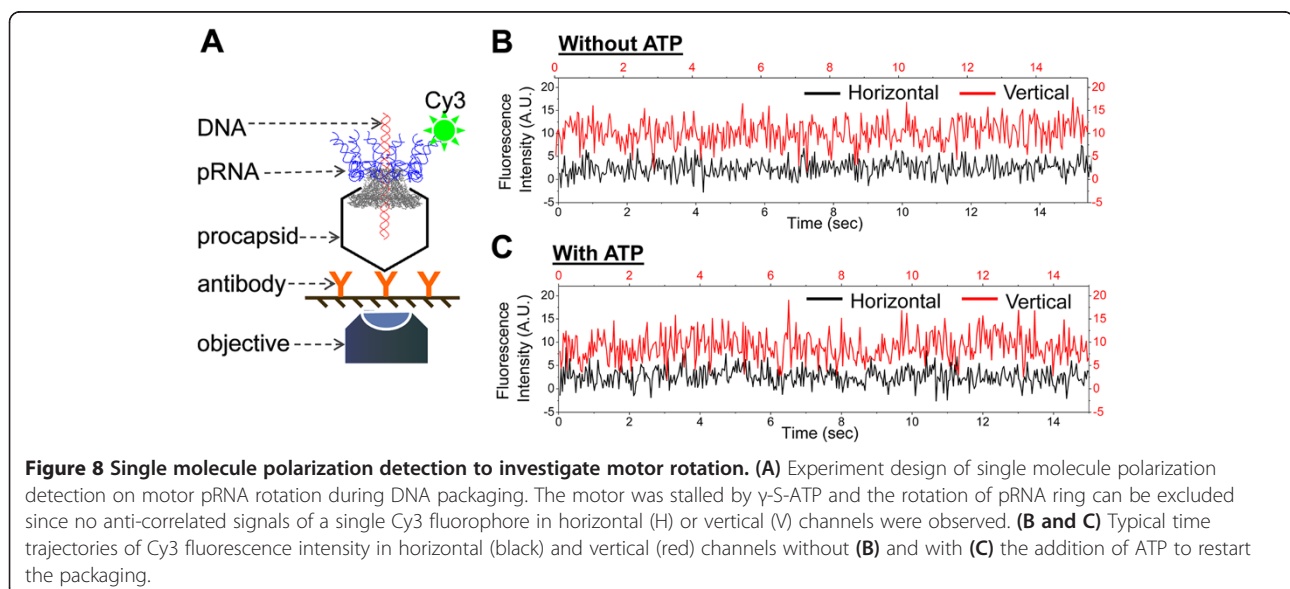
and restructuring of the connector core subunit are promoted by the interactions among Phi29 DNA and its structural proteins [95]. Due to the dsDNA alignment with the channel wall [9,10,50,53,54] and the relatively static C-terminal internal region, a significant conformational shift in the N-terminal external region then results in a clockwise twist of the dsDNA when viewed from the C-terminus (Figure 6).

Recently, it has been reported that a small angular twist of 1.5 degree per nucleotide was observed during dsDNA packaging in Phi29 [97]. Observation of such a small angular deviation per nucleotide can be explained by these conformational changes of the connector (Figure 6). As evidenced above [95], if the N-terminal external region is shifted more significantly than the internal C-terminal region, a leftward twist of the DNA will occur during revolution along the connector channel (Figure 6B). This is in agreement with the observed clockwise twist of 1.5 degree per nucleotide relative to the C-terminus of the connector [97]. The reported twist of 1.5 degree per nucleotide or 15.75° per helical pitch of 10.5 bp [97] during dsDNA packaging cannot be taken as rotation mechanism in which 360° per pitch or ~34° per base pair are required. Furthermore, the reported increase in the frequency of DNA twisting per nucleotide with increase in capsid filling, is in agreement with the observation that the conformational change of the channel accelerates towards the end of the packaging process [96] (Figure 6A). This is logical since the dsDNA is aligned with the wall of the connector channel, and when DNA packaging is close to completion, a final conformation will be adopted and a more obvious twisting will be observed to prepare the channel for DNA ejection toward host infection.

Single-molecule real-time imaging and force spectroscopy revealed that no rotation occurs during DNA translocation

In order to validate the model of revolution without the need for rotation, several single-molecule imaging experiments were carried out (Figures 7 and 8). A micrometer-sized fluorescence bead was attached to the distal end of the Phi29 genomic dsDNA. DNA translocation was directly observed in real-time by single-molecule imaging microscopy to detect fluorescence images revealing the displacement of the bead [49,51]. No rotation was found in these traces (Figure 7). To exclude the possibility that the lack of rotation is a result of bond freedom between the beads and DNA or due to the difficulty in optical discrimination due to the spherical nature of the beads, a cluster of magnetic beads was attached to the end of the Phi29 DNA to generate a label with an asymmetric shape (Figure 7B) [49]. Experiments using different setups for DNA packaging in a vertical (Figure 7A) and horizontal orientation (Figure 7B) [49] have been repeated many times and no rotation of DNA was observed. Polarization studies have been used to study biomotors such as T4 helicase [72]. The polarization analysis of Phi29 DNA packaging motor did not find a rotation phenomenon either (Figure 8).

The mechanism where no DNA rotation is required during packaging is further supported by the observation that in bacteriophage T4, both DNA ends are tethered to the portal throughout DNA packaging once the packaged DNA persistence length of about 500 bp is reached, suggesting that no rotation is needed and DNA does not get tangled up [87,98]. All these observations support a revolution mechanism for phage DNA packaging without the need for rotation.



Conclusion

The revolution mechanism is a common feature shared by many DNA translocation motors. Inspections of structural data from eukaryotic and prokaryotic dsDNA translocases suggest that revolution and rotation motors can be distinguished by measuring the size and chirality of the DNA translocation channel. The channel of revolution motors are larger than 3 nm, while the channels of rotation motors are smaller than 2 nm in diameter. Revolution motors use a left-handed channel to drive the right-handed dsDNA in an anti-chiral arrangement, while some rotation motors use parallel threads with a right-handed channel. Revolution motors hold both strands of the dsDNA within the channel, while some rotation motor hold only one strand of the DNA inside the channel [5,64,67,69-71]. Such revolution motors are void of dsDNA coiling [9,50,54,55]. A small-angle left-handed twist of dsDNA, which is aligned with the channel, takes place due to the conformational shifts of the motor channel from a left-handed configuration for DNA entry to a right-handed configuration for DNA ejection for host cell infection, however, no dsDNA rotation is required for DNA packaging.

Materials and methods

Incorporation of the connector channel into a planar bilayer lipid membrane

The method of inserting the connector with reconstituted liposomes into a lipid bilayer has been reported previously [99]. Briefly, a Teflon film partition (aperture 200 μ m in diameter) was used to separate a bilayer lipid membrane chamber (BLM) into *cis*- and *trans*- compartments. The aperture was painted two times with 0.5 μ L of 3% (w/v) DPhPC n-decane solution, and the two compartments were filled with conducting buffer (1 M NaCl or 1 M KCl, 5 mM HEPES, pH 7.4). After formation of the lipid bilayer on the aperture, the lipid/connector complexes were added to the chamber and allowed to fuse with the planar lipid bilayer.

Construction of tetra-stranded DNA

Five strands were custom ordered from IDT, with the following sequences: Strand-1: 5'-CGC AGA CAT CCT GCC GTA GCC TGA GGC ACA CG-3'; Strand-2: 5'-CGT GTG CCT CAC CGA CCA ATG C-3'; Strand-3: 5'-GCA TTG GTC GGA CTG AAC AGG ACT ACG CTG GC-3'; Strand-4: 5'-GCC AGC GTA GTG GAT GTC TGC G-3'; Strand-5: 5'-TC AGT GGC TAC GGC ACC GT-3'. The five strands were annealed in stoichiometric ratio in TMS (Tris-magnesium saline) buffer (50 mM Tris-HCl, pH8.0, 100 mM NaCl and 10 mM MgCl₂) and purified in 12% (w/v) native PAGE, following reported procedures [100].

Single channel conduction assays for each membrane inserted connector channels

A pair of Ag/AgCl electrodes was connected directly into the *cis*- and *trans*- compartments to measure the current traces across the lipid bilayer membrane. The current trace was recorded using an Axopatch 200B patch clamp amplifier coupled with the Axon DigiData 1322A analog-digital converter (Axon Instruments) or the BLM workstation (Warner Instruments). All voltages reported were those of the *trans*- compartment. Data was low band-pass filtered at a frequency of 1 kHz, and acquired at a sampling frequency of 10–100 kHz. The Patch clamp 9.1 software (Axon Instruments) was used to collect the data, and the software Origin Pro 8.0 was used to analyze all the data.

Direct observation of DNA translocation

The stalled packaging intermediates containing biotinylated DNA were prepared by using non-hydrolyzable γ -S-ATP [101]. The intermediates were then immobilized to perfusion chambers built from glass slides and coverslips (Figure 7). The 0.53 μ m fluorescent streptavidin microspheres (Bangs Laboratories Inc.) were bound to the protruding, biotinylated DNA end of the intermediates. After restarting the packaging reaction by adding gp16 and ATP [101], an individual DNA-packaging event was observed. Epi-illumination was used. Sequential images with 8-bit digital resolution were recorded at 1 frame per second for 600 s. The pixel resolution of the images was 0.26 μ m/pixel.

Abbreviations

DsDNA: Double stranded DNA; ASCE: Additional strand catalytic E; EMSA: Electrophoretic mobility shift assays; smFRET: Single molecule fluorescence resonance energy transfer.

Competing interests

Peixuan Guo is a co-founder of Kylin Therapeutics, Inc., and Biomotor and RNA Nanotech Development Co. Ltd.

Authors' contributions

GMDD, ZZ, LH, FH and CS carried out the experiments and participate the manuscript preparation. HZ carried out the single-molecule experiments. SW carried out the sequence alignment. OT participated in the data analysis. PG conceived the concept, designed the experiment and wrote the manuscript. All authors read and approved the final manuscript.

Authors' information

Gian Marco De-Donatis and Zhengyi Zhao serve as co-first author.

Acknowledgements

We would like to thank Dr. Guo-Min Li for his valuable comments. The work was supported by NIH grants R01 EB012135. The content is solely the responsibility of the authors and does not necessarily represent the official views of NIH. Funding to Peixuan Guo's Endowed Chair in Nanobiotechnology position is from the William Fairish Endowment Fund. PG is a cofounder of Kylin Therapeutics, Inc., and Biomotor and RNA Nanotech Development Co. Ltd.

Author details

¹Nanobiotechnology Center, University of Kentucky, Lexington, KY, USA. ²Department of Pharmaceutical Sciences, College of Pharmacy, University of Kentucky, Lexington, KY, USA. ³Markey Cancer Center, University of Kentucky,

Lexington, KY, USA. ⁴Current address: Institute for Biomarker Research, Medical Diagnostic Laboratories, L.L.C., Hamilton, NJ 08690, USA. ⁵William Farish Endowed Chair in Nanobiotechnology, School of Pharmacy, University of Kentucky, 565 Biopharmaceutical Complex, 789 S. Limestone Street, Lexington, KY 40536, USA.

Received: 14 April 2014 Accepted: 16 May 2014

Published: 1 June 2014

References

- Snider J, Houry WA: **AAA + proteins: diversity in function, similarity in structure.** *Biochem Soc Trans* 2008, **36**:72–77.
- Ammelburg M, Frickey T, Lupas AN: **Classification of AAA + proteins.** *J Struct Biol* 2006, **156**:2–11.
- White SR, Lauring B: **AAA + ATPases: Achieving diversity of function with conserved machinery.** *Traffic* 2007, **8**:1657–1667.
- Chen YJ, Yu X, Egelman EH: **The hexameric ring structure of the Escherichia coli RuvB branch migration protein.** *J Mol Biol* 2002, **319**:587–591.
- Singleton MR, Dillingham MS, Wigley DB: **Structure and mechanism of helicases and nucleic acid translocases.** *Ann Rev Biochem* 2007, **76**:23–50.
- Kainov DE, Tuma R, Mancini EJ: **Hexameric molecular motors: P4 packaging ATPase unravels the mechanism.** *Cell Mol Life Sci* 2006, **63**(10):1095–1105.
- Hanson PI, Whiteheart SW: **AAA + proteins: have engine, will work.** *Nat Rev Mol Cell Biol* 2005, **6**:519–529.
- Schwartz C, Fang H, Huang L, Guo P: **Sequential action of ATPase, ATP, ADP, Pi and dsDNA in procapsid-free system to enlighten mechanism in viral dsDNA packaging.** *Nucleic Acids Res* 2012, **40**:2577–2586.
- Guo P, Schwartz C, Haak J, Zhao Z: **Discovery of a new motion mechanism of biomotors similar to the earth revolving around the sun without rotation.** *Virology* 2013, **446**:133–143.
- Guo P, Zhao Z, Haak J, Wang S, Weitao T: **Common mechanisms of DNA translocation motors in bacteria and viruses using one-way revolution mechanism without rotation.** *Biotechnol Adv* 2014. In Press.
- Zhang YB, Yuan FH, Presnell SR, Tian KL, Gao Y, Tomkinson AE, Gu LY, Li GM: **Reconstitution of 5'-directed human mismatch repair in a purified system.** *Cell* 2005, **122**:693–705.
- Binzel DW, Khisamutdinov EF, Guo P: **Entropy-Driven One-Step Formation of Phi29 pRNA 3WJ from Three RNA Fragments.** *Biochemistry* 2014, **53**:2221–2231.
- Khisamutdinov EF, Jasinski DL, Guo P: **RNA as a Boiling-Resistant Anionic Polymer Material To Build Robust Structures with Defined Shape and Stoichiometry.** *ACS Nano* 2014. In press. DOI: 10.1021/nn5006254.
- Fang H, Zhang P, Huang LP, Zhao Z, Pi F, Montemagno C, Guo P: **Binomial distribution for quantification of protein subunits in biological nanoassemblies and functional nanomachines.** *Nanomedicine* 2014. In press. DOI: 10.1016/j.nano.2014.03.005.
- Zhang H, Guo P: **Single molecule photobleaching (SMPB) technology for counting of RNA, DNA, protein and other molecules in nanoparticles and biological complexes by TIRF instrumentation.** *Methods* 2014, **67**(2):169–176.
- Zhang H, Endrizzi JA, Shu Y, Haque F, Sauter C, Shlyakhtenko LS, Lyubchenko Y, Guo P, Chi YL: **Crystal structure of 3WJ core revealing divalent ion-promoted thermostability and assembly of the Phi29 Hexameric motor pRNA.** *RNA* 2013, **19**:1226–1237.
- Shu Y, Shu D, Haque F, Guo P: **Fabrication of pRNA nanoparticles to deliver therapeutic RNAs and bioactive compounds into tumor cells.** *Nat Protoc* 2013, **8**:1635–1659.
- Xiao F, Zhang H, Guo P: **Novel mechanism of hexamer ring assembly in protein/RNA interactions revealed by single molecule imaging.** *Nucleic Acids Res* 2008, **36**:6620–6632.
- Xiao F, Sun J, Coban O, Schoen P, Wang JC, Cheng RH, Guo P: **Fabrication of massive sheets of single layer patterned arrays using lipid directed reengineered Phi29 motor Dodecamer.** *ACS Nano* 2009, **3**:100–107.
- Xiao F, Demeler B, Guo P: **Assembly mechanism of the sixty-subunit nanoparticles via interaction of RNA with the reengineered protein connector of phi29 DNA-packaging motor.** *ACS Nano* 2010, **4**:3293–3301.
- Mehta A: **Myosin learns to walk.** *J Cell Sci* 2001, **114**:1981–1998.
- Visscher K, Schnitzer MJ, Block SM: **Single kinesin molecules studied with a molecular force clamp.** *Nature* 1999, **400**:184–189.
- Vale RD, Funatsu T, Pierce DW, Romberg L, Harada Y, Yanagida T: **Direct observation of single kinesin molecules moving along microtubules.** *Nature* 1996, **380**:451–453.
- Harada Y, Ohara O, Takatsuki A, Itoh H, Shimamoto N, Kinosita K Jr: **Direct observation of DNA rotation during transcription by Escherichia coli RNA polymerase.** *Nature* 2001, **409**:113–115.
- Doering C, Ermentrout B, Oster G: **Rotary DNA motors.** *Biophys J* 1998, **69**:2256–2267.
- Ariga T, Masaike T, Noji H, Yoshida M: **Stepping rotation of F(1)-ATPase with one, two, or three altered catalytic sites that bind ATP only slowly.** *J Biol Chem* 2002, **277**:24870–24874.
- Casjens SR: **The DNA-packaging nanomotor of tailed bacteriophages.** *Nat Rev Microbiol* 2011, **9**:647–657.
- Roos WH, Ivanovska IL, Evilevitch A, Wuite GJL: **Viral capsids: mechanical characteristics, genome packaging and delivery mechanisms.** *Cell Mol Life Sci* 2007, **64**:1484–1497.
- Catalano CE: **The terminase enzyme from bacteriophage lambda: a DNA-packaging machine.** *Cell Mol Life Sci* 2000, **57**:128–148.
- Hendrix RW: **Bacteriophage DNA packaging: RNA gears in a DNA transport machine (Minireview).** *Cell* 1998, **94**:147–150.
- Guo PX, Lee TJ: **Viral nanomotors for packaging of dsDNA and dsRNA.** *Mol Microbiol* 2007, **64**:886–903.
- Zhang H, Schwartz C, De Donatis GM, Guo P: **"Push Through One-Way Valve" mechanism of viral DNA packaging.** *Adv Virus Res* 2012, **83**:415–465.
- Serwer P: **A hypothesis for bacteriophage DNA packaging motors.** *Viruses* 2010, **2**:1821–1843.
- Guo P, Peterson C, Anderson D: **Prohead and DNA-gp3-dependent ATPase activity of the DNA packaging protein gp16 of bacteriophage phi29.** *J Mol Biol* 1987, **197**:229–236.
- Sabanayagam CR, Oram M, Lakowicz JR, Black LW: **Viral DNA packaging studied by fluorescence correlation spectroscopy.** *Biophys J* 2007, **93**:L17–L19.
- Hwang JS, Bogner E: **ATPase activity of the terminase subunit pUL56 of human cytomegalovirus.** *J Biol Chem* 2002, **277**:6943–6948.
- Gual A, Camacho AG, Alonso JC: **Functional analysis of the terminase large subunit, G2P, of Bacillus subtilis bacteriophage SPP1.** *J Biol Chem* 2000, **275**:35311–35319.
- Hang JQ, Tack BF, Feiss M: **ATPase center of bacteriophage lambda terminase involved in post-cleavage stages of DNA packaging: identification of ATP-interactive amino acids.** *J Mol Biol* 2000, **302**:777–795.
- Hwang Y, Catalano CE, Feiss M: **Kinetic and mutational dissection of the two ATPase activities of terminase, the DNA packaging enzyme of bacteriophage lambda.** *Biochemistry* 1996, **35**:2796–2803.
- Rubinchik S, Parris W, Gold M: **The in-vitro ATPases of bacteriophage-lambda terminase and its large subunit, gene product A. The relationship with their DNA helicase and packaging activities.** *J Biol Chem* 1994, **269**:13586–13593.
- Morita M, Tasaka M, Fujisawa H: **DNA packaging ATPase of bacteriophage T3.** *Virology* 1993, **193**:748–752.
- Koonin EV, Senkevich TG, Chernov VI: **Gene-A32 product of vaccinia virus may be an ATPase involved in viral-DNA packaging as indicated by sequence comparisons with other putative viral ATPases.** *Virus Genes* 1993, **7**:89–94.
- Hendrix RW: **Symmetry mismatch and DNA packaging in large bacteriophages.** *Proc Natl Acad Sci U S A* 1978, **75**:4779–4783.
- Valpuesta JM, Carrascosa J: **Structure of viral connectors and their function in bacteriophage assembly and DNA packaging.** *Q Rev Biophys* 1994, **27**:107–155.
- Olia AS, Prevelige PE, Johnson JE, Cingolani G: **Three-dimensional structure of a viral genome-delivery portal vertex.** *Nat Struct Mol Biol* 2011, **18**:597–603.
- Guasch A, Pous J, Ibarra B, Gomis-Ruth FX, Valpuesta JM, Sousa N, Carrascosa JL, Coll M: **Detailed architecture of a DNA translocating machine: the high-resolution structure of the bacteriophage phi29 connector particle.** *J Mol Biol* 2002, **315**:663–676.
- Baumann RG, Mullaney J, Black LW: **Portal fusion protein constraints on function in DNA packaging of bacteriophage T4.** *Mol Microbiol* 2006, **61**:16–32.
- Hugel T, Michaelis J, Hetherington CL, Jardine PJ, Grimes S, Walter JM, Faik W, Anderson DL, Bustamante C: **Experimental test of connector rotation during DNA packaging into bacteriophage phi29 capsids.** *PLoS Biol* 2007, **5**:558–567.

49. Chang C, Zhang H, Shu D, Guo P, Savran C: **Bright-field analysis of phi29 DNA packaging motor using a magnetomechanical system.** *Appl Phys Lett* 2008, **93**:153902–153903.
50. Schwartz C, De Donatis GM, Zhang H, Fang H, Guo P: **Revolution rather than rotation of AAA+ hexameric phi29 nanomotor for viral dsDNA packaging without coiling.** *Virology* 2013, **443**:28–39.
51. Shu D, Zhang H, Jin J, Guo P: **Counting of six pRNAs of phi29 DNA-packaging motor with customized single molecule dual-view system.** *EMBO J* 2007, **26**:527–537.
52. Jing P, Haque F, Shu D, Montemagno C, Guo P: **One-way traffic of a viral motor channel for double-stranded DNA translocation.** *Nano Lett* 2010, **10**:3620–3627.
53. Schwartz C, De Donatis GM, Fang H, Guo P: **The ATPase of the phi29 DNA-packaging motor is a member of the hexameric AAA+ superfamily.** *Virology* 2013, **443**:20–27.
54. Zhao Z, Khisamutdinov E, Schwartz C, Guo P: **Mechanism of one-way traffic of hexameric phi29 DNA packaging motor with four electropositive relaying layers facilitating anti-parallel revolution.** *ACS Nano* 2013, **7**:4082–4092.
55. Guo P: **Biophysical studies reveal new evidence for one-way revolution mechanism of bacteriophage varphi29 DNA packaging motor.** *Biophys J* 2014, **106**:1837–1838.
56. Demarre G, Galli E, Barre FX: **The FtsK family of DNA pumps.** *Adv Exp Med Biol* 2013, **767**:245–262.
57. Barre FX: **FtsK and SpoIIIE: the tale of the conserved tails.** *Mol Microbiol* 2007, **66**:1051–1055.
58. Crozat E, Grainge I: **FtsK DNA translocase: the fast motor that knows where it's going.** *ChemBiochem* 2010, **11**:2232–2243.
59. Bath J, Wu LJ, Errington J, Wang JC: **Role of Bacillus subtilis SpoIIIE in DNA transport across the mother cell-prespore division septum.** *Science* 2000, **290**:995–997.
60. Massey TH, Mercogliano CP, Yates J, Sherratt DJ, Lowe J: **Double-stranded DNA translocation: structure and mechanism of hexameric FtsK.** *Mol Cell* 2006, **23**:457–469.
61. Pease PJ, Levy O, Cost GJ, Gore J, Ptacin JL, Sherratt D, Bustamante C, Cozzarelli NR: **Sequence-directed DNA translocation by purified FtsK.** *Science* 2005, **307**:586–590.
62. Saleh OA, Bigot S, Barre FX, Allemand JF: **Analysis of DNA supercoil induction by FtsK indicates translocation without groove-tracking.** *Nat Struct Mol Biol* 2005, **12**:436–440.
63. Iyer LM, Makarova KS, Koonin EV, Aravind L: **Comparative genomics of the FtsK-HerA superfamily of pumping ATPases: implications for the origins of chromosome segregation, cell division and viral capsid packaging.** *Nucleic Acids Res* 2004, **32**:5260–5279.
64. Bianco P, Kowalczykowski S: **Translocation step size and mechanism of the RecBC DNA helicase.** *Nature* 2000, **405**:368–372.
65. Lebedev AA, Krause MH, Isidro AL, Vagin AA, Orlova EV, Turner J, Dodson EJ, Tavares P, Antson AA: **Structural framework for DNA translocation via the viral portal protein.** *EMBO J* 2007, **26**:1984–1994.
66. Sun S, Kondabagil K, Draper B, Alam TI, Bowman VD, Zhang Z, Hegde S, Fokine A, Rossmann MG, Rao VB: **The structure of the phage T4 DNA packaging motor suggests a mechanism dependent on electrostatic forces.** *Cell* 2008, **135**:1251–1262.
67. Enemark EJ, Joshua-Tor L: **On helicases and other motor proteins.** *Curr Opin Struct Biol* 2008, **18**:243–257.
68. Patel SS, Picha KM: **Structure and function of hexameric helicases.** *Annu Rev Biochem* 2000, **69**:651–697.
69. Itsathitphaisarn O, Wing RA, Eliason WK, Wang J, Steitz TA: **The hexameric helicase DnaB adopts a nonplanar conformation during translocation.** *Cell* 2012, **151**:267–277.
70. Hacker KJ, Johnson KA: **A hexameric helicase encircles one DNA strand and excludes the other during DNA unwinding.** *Biochemistry* 1997, **36**:14080–14087.
71. Dittrich M, Schulten K: **PcrA helicase, a prototype ATP-driven molecular motor.** *Structure* 2006, **14**:1345–1353.
72. Phelps C, Lee W, Jose D, von Hippel PH, Marcus AH: **Single-molecule FRET and linear dichroism studies of DNA breathing and helicase binding at replication fork junctions.** *Proc Natl Acad Sci U S A* 2013, **110**:17320–17325.
73. Fei J, Ha T: **Watching DNA breath one molecule at a time.** *Proc Natl Acad Sci U S A* 2013, **110**:17173–17174.
74. Lee W, Jose D, Phelps C, Marcus AH, von Hippel PH: **A single-molecule view of the assembly pathway, subunit stoichiometry, and unwinding activity of the bacteriophage T4 primosome (helicase-primase) complex.** *Biochemistry* 2013, **52**:3157–3170.
75. Agirrezabala X, Martin-Benito J, Valle M, Gonzalez JM, Valencia A, Valpuesta JM, Carrascosa JL: **Structure of the connector of bacteriophage T7 at 8Å resolution: structural homologies of a basic component of a DNA translocating machinery.** *J Mol Biol* 2005, **347**:895–902.
76. Xing X, Bell CE: **Crystal structures of Escherichia coli RecA in a compressed helical filament.** *J Mol Biol* 2004, **342**:1471–1485.
77. Pascal JM, Tsodikov OV, Hura GL, Song W, Cotner EA, Classen S, Tomkinson AE, Tainer JA, Ellenberger T: **A flexible interface between DNA ligase and PCNA supports conformational switching and efficient ligation of DNA.** *Mol Cell* 2006, **24**:279–291.
78. Bailey S, Eliason WK, Steitz TA: **Structure of hexameric DnaB helicase and its complex with a domain of DnaG primase.** *Science* 2007, **318**:459–463.
79. Enemark EJ, Joshua-Tor L: **Mechanism of DNA translocation in a replicative hexameric helicase.** *Nature* 2006, **442**:270–275.
80. Gomis-Ruth FX, Coll M: **Structure of TrwB, a gatekeeper in bacterial conjugation.** *Int J Biochem Cell Biol* 2001, **33**:839–843.
81. Burroughs AM, Iyer LM, Aravind L: **Comparative genomics and evolutionary trajectories of viral atp dependent DNA-packaging systems.** *Genome Dyn* 2007, **3**:48–65.
82. Chelikani V, Ranjan T, Zade A, Shukla A, Kondabagil K: **Genome segregation and packaging machinery in acanthamoeba polyphaga mimivirus is reminiscent of bacterial apparatus.** *J Virol* 2014, **88**:6069–6075.
83. Guo F, Liu Z, Vago F, Ren Y, Wu W, Wright ET, Serwer P, Jiang W: **Visualization of uncorrelated, tandem symmetry mismatches in the internal genome packaging apparatus of bacteriophage T7.** *Proc Natl Acad Sci U S A* 2013, **110**:6811–6816.
84. Pearson RK, Fox MS: **Effects of DNA heterologies on bacteriophage lambda packaging.** *Genetics* 1988, **118**:5–12.
85. Moll W-D, Guo P: **Translocation of nicked but not gapped DNA by the packaging motor of bacteriophage phi29.** *J Mol Biol* 2005, **351**:100–107.
86. Aathavan K, Politzer AT, Kaplan A, Moffitt JR, Chemla YR, Grimes S, Jardine PJ, Anderson DL, Bustamante C: **Substrate interactions and promiscuity in a viral DNA packaging motor.** *Nature* 2009, **461**:669–673.
87. Oram M, Sabanayagam C, Black LW: **Modulation of the packaging reaction of bacteriophage T4 terminase by DNA structure.** *J Mol Biol* 2008, **381**:61–72.
88. Simpson AA, Tao Y, Leiman PG, Badasso MO, He Y, Jardine PJ, Olson NH, Morais MC, Grimes S, Anderson DL, Baker TS, Rossmann MG: **Structure of the bacteriophage phi29 DNA packaging motor.** *Nature* 2000, **408**:745–750.
89. Fang H, Jing P, Haque F, Guo P: **Role of channel Lysines and "Push Through a One-way Valve" mechanism of viral DNA packaging motor.** *Biophys J* 2012, **102**:127–135.
90. Grimes S, Ma S, Gao J, Atz R, Jardine PJ: **Role of phi29 connector channel loops in late-stage DNA packaging.** *J Mol Biol* 2011, **410**:50–59.
91. Lander GC, Tang L, Casjens SR, Gilcrease EB, Prevelige P, Poliakov A, Potter CS, Carragher B, Johnson JE: **The structure of an infectious P22 virion shows the signal for headful DNA packaging.** *Science* 2006, **312**:1791–1795.
92. Molineux IJ, Panja D: **Popping the cork: mechanisms of phage genome ejection.** *Nat Rev Microbiol* 2013, **11**:194–204.
93. Petrov AS, Harvey SC: **Packaging double-helical DNA into viral capsids: structures, forces, and energetics.** *Biophys J* 2008, **95**:497–502.
94. Jiang W, Chang J, Jakana J, Weigele P, King J, Chiu W: **Structure of epsilon15 bacteriophage reveals genome organization and DNA packaging/injection apparatus.** *Nature* 2006, **439**:612–616.
95. Tang JH, Olson N, Jardine PJ, Grimes S, Anderson DL, Baker TS: **DNA poised for release in bacteriophage phi29.** *Structure* 2008, **16**:935–943.
96. Geng J, Fang H, Haque F, Zhang L, Guo P: **Three reversible and controllable discrete steps of channel gating of a viral DNA packaging motor.** *Biomaterials* 2011, **32**:8234–8242.
97. Liu S, Chistol G, Hetherington CL, Tafaya S, Aathavan K, Schnitzbauer J, Grimes S, Jardine PJ, Bustamante C: **A viral packaging motor varies its DNA rotation and step size to preserve subunit coordination as the capsid fills.** *Cell* 2014, **157**:702–713.
98. Ray K, Ma J, Oram M, Lakowicz JR, Black LW: **Single-molecule and FRET fluorescence correlation spectroscopy analyses of phage DNA**

packaging: colocalization of packaged phage T4 DNA ends within the capsid. *J Mol Biol* 2010, **395**:1102–1113.

99. Wendell D, Jing P, Geng J, Subramaniam V, Lee TJ, Montemagno C, Guo P: Translocation of double-stranded DNA through membrane-adapted phi29 motor protein nanopores. *Nat Nanotechnol* 2009, **4**:765–772.
100. Li X, Yang X, Qi J, Seeman N: Antiparallel DNA double crossover molecules as components for nanoconstruction. *J Am Chem Soc* 1996, **118**:6131–6140.
101. Shu D, Guo P: Only one pRNA hexamer but multiple copies of the DNA-packaging protein gp16 are needed for the motor to package bacterial virus phi29 genomic DNA. *Virology* 2003, **309**(1):108–113.

doi:10.1186/2045-3701-4-30

Cite this article as: De-Donatis *et al.*: Finding of widespread viral and bacterial revolution dsDNA translocation motors distinct from rotation motors by channel chirality and size. *Cell & Bioscience* 2014 **4**:30.

**Submit your next manuscript to BioMed Central
and take full advantage of:**

- Convenient online submission
- Thorough peer review
- No space constraints or color figure charges
- Immediate publication on acceptance
- Inclusion in PubMed, CAS, Scopus and Google Scholar
- Research which is freely available for redistribution

Submit your manuscript at
www.biomedcentral.com/submit

